

# Possibility to locate the position of the H<sub>2</sub>O snowline in protoplanetary disks through spectroscopic observations

Shota Notsu<sup>1,2</sup>, Hideko Nomura<sup>3</sup>, Catherine Walsh<sup>4</sup>,  
Mitsuhiko Honda<sup>5</sup>, Tomoya Hirota<sup>6</sup>, Eiji Akiyama<sup>6</sup> and T. J. Millar<sup>7</sup>

<sup>1</sup>Department of Astronomy, Graduate School of Science, Kyoto University,  
Kitashirakawa-Oiwake-cho, Sakyo-ku, Kyoto 606-8502, Japan  
e-mail: snotsu@kusastro.kyoto-u.ac.jp

<sup>2</sup>Research Fellow of Japan Society for the Promotion of Science (DC1)

<sup>3</sup>Department of Earth and Planetary Science, Tokyo Institute of Technology, 2-12-1  
Ookayama, Meguro-ku, Tokyo 152-8551, Japan

<sup>4</sup>School of Physics and Astronomy, University of Leeds, Leeds, LS2 9JT, UK

<sup>5</sup>Department of Physics, School of Medicine, Kurume University, 67 Asahi-machi, Kurume,  
Fukuoka 830-0011, Japan

<sup>6</sup>National Astronomical Observatory of Japan, 2-21-1 Osawa, Mitaka, Tokyo 181-8588, Japan

<sup>7</sup>Astrophysics Research Centre, School of Mathematics and Physics, Queen's University  
Belfast, University Road, Belfast, BT7 1NN, UK

**Abstract.** Observationally measuring the location of the H<sub>2</sub>O snowline is crucial for understanding the planetesimal and planet formation processes, and the origin of water on Earth. The velocity profiles of emission lines from protoplanetary disks are usually affected by Doppler shift due to Keplerian rotation and thermal broadening. Therefore, the velocity profiles are sensitive to the radial distribution of the line-emitting regions. In our work (Notsu *et al.* 2016, 2017), we found candidate water lines to locate the position of the H<sub>2</sub>O snowline through future high-dispersion spectroscopic observations. First, we calculated the chemical composition of the disks around a T Tauri star and a Herbig Ae star using chemical kinetics. We confirmed that the abundance of H<sub>2</sub>O gas is high not only in the hot midplane region inside the H<sub>2</sub>O snowline but also in the hot surface layer and the photodesorption region of the outer disk. The position of the H<sub>2</sub>O snowline in the Herbig Ae disk exists at a larger radius from the central star than that in the T Tauri disk. Second, we calculated the H<sub>2</sub>O line profiles and identified that H<sub>2</sub>O emission lines with small Einstein *A* coefficients ( $\sim 10^{-6} - 10^{-3} \text{ s}^{-1}$ ) and relatively high upper state energies ( $\sim 1000\text{K}$ ) are dominated by emission from the hot midplane region inside the H<sub>2</sub>O snowline, and therefore their profiles potentially contain information which can be used to locate the position of the H<sub>2</sub>O snowline. The wavelengths of the H<sub>2</sub>O lines which are the best candidates to locate the position of the H<sub>2</sub>O snowline range from mid-infrared to sub-millimeter, and the total line fluxes tend to increase with decreasing wavelengths. We investigated the possibility of future observations using the ALMA and mid-infrared high-dispersion spectrographs (e.g., SPICA/SMI-HRS). Since the fluxes of those identified lines from a Herbig Ae disk are stronger than those of a T Tauri disk, the possibility of a successful detection is expected to increase for a Herbig Ae disk.

---

## 1. Introduction

Observationally locating the position of the H<sub>2</sub>O snowline (Hayashi 1981; Hayashi *et al.* 1985) in a protoplanetary disk is important. It will provide information on the physical and chemical conditions in disks, such as the temperature structure, the dust-grain size distribution, and the water vapor distribution in the disk midplane (e.g., Oka *et al.*

2011; Piso *et al.* 2015), and will give constraints on the current formation theories of planetesimals and planets (e.g., Öberg *et al.* 2011; Okuzumi *et al.* 2012; Ros & Johansen 2013). It will help clarify the origin of water on rocky planets including the Earth (e.g., Morbidelli *et al.* 2000, 2012, 2016; Sato *et al.* 2016). Through recent space and ground infrared spectroscopic observations for protoplanetary disks, some infrared H<sub>2</sub>O lines, which mainly trace the disk surface and the photodesorption region of the outer disk, have been detected (for more details, see e.g., Pontoppidan *et al.* 2010a,b; Hogerheijde *et al.* 2011; van Dishoeck *et al.* 2014; Blevins *et al.* 2016; Banzatti *et al.* 2017; Notsu *et al.* 2016, 2017).

The velocity profiles of emission lines from protoplanetary disks are usually affected by Doppler shift due to Keplerian rotation and thermal broadening. Therefore, the velocity profiles are sensitive to the radial distribution of the line-emitting regions. In our work (e.g., Notsu *et al.* 2016, 2017), we calculated the chemical composition and the H<sub>2</sub>O line profiles in a T Tauri disk† and a Herbig Ae disk. We investigated the line properties in detail for candidate water lines to locate the position of the H<sub>2</sub>O snowline over a wide wavelength range from mid-infrared to sub-millimeter, and discuss the possibility of detecting such lines with future observations. In this proceeding paper, we introduce the outline and key results of our recent work (Notsu *et al.* 2016, 2017).

## 2. Method & Result

### 2.1. *The physical models of the protoplanetary disks*

The physical structures of the protoplanetary disk models used here are calculated using the methods in Nomura & Millar (2005) including X-ray heating (Nomura *et al.* 2007). A more detailed description of the background theory and computation of this physical model is described in the original papers (Nomura & Millar 2005; Nomura *et al.* 2007) and our works (e.g., Notsu *et al.* 2015, 2016, 2017). Walsh *et al.* (2010, 2012, 2014, 2015), Heinzeller *et al.* (2011), Furuya *et al.* (2013) used the same physical models for a T Tauri disk and a Herbig Ae disk to study various chemical and physical effects, and they also describe the calculation of the physical structures in detail.

We adopted the physical models of a steady, axisymmetric Keplerian disks surrounding a T Tauri star with mass  $M_* = 0.5M_\odot$ , radius  $R_* = 2.0R_\odot$ , and effective temperature  $T_* = 4000\text{K}$ , and a Herbig Ae star with  $M_* = 2.5M_\odot$ ,  $R_* = 2.0R_\odot$ , and  $T_* = 10,000\text{K}$ . We adopt the same compact and spherical dust-grain model of Nomura & Millar (2005). In Figure 1, we display the gas number density and the gas temperature of a Herbig Ae disk (Notsu *et al.* 2017).

### 2.2. *Chemical structures of the protoplanetary disks*

To investigate the chemical structure of disks, we use a large chemical network which includes gas-phase reactions and gas-grain interactions (freeze-out of gas molecules on dust grains, and thermal and non-thermal desorption from dust grains). The initial fractional abundances (relative to total hydrogen nuclei density) we use are atomic and oxygen-rich low-metallicity from Graedel *et al.* (1982), listed in Table 8 of Woodall *et al.* (2007).

Figure 2 shows the fractional abundances (relative to total gas hydrogen nuclei density,  $n_{\text{H}}$ ) of H<sub>2</sub>O gas and ice in a Herbig Ae disk (Notsu *et al.* 2017). The H<sub>2</sub>O snowline of the Herbig Ae disk exists at a radius of  $r \sim 14$  au in the midplane ( $\sim 120\text{K}$ ), which is significantly larger than that for the T Tauri disk model ( $r \sim 1.6$  au, see Figure 2 of

† In the remainder of this paper, we define the protoplanetary disks around T Tauri/Herbig Ae stars as “T Tauri/Herbig Ae disks”.

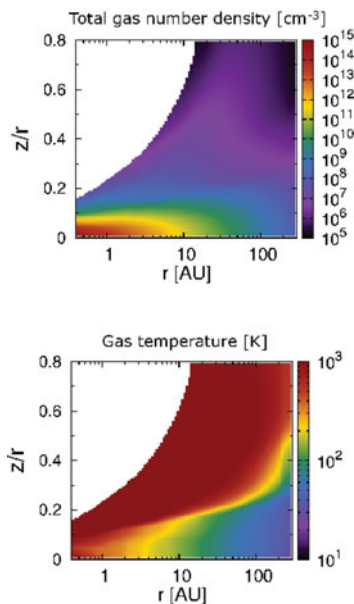


**Figure 1.** The total gas number density in  $\text{cm}^{-3}$  (top), the gas temperature in Kelvin (bottom) of a Herbig Ae disk as a function of the disk radius in au and height (scaled by the radius,  $z/r$ ) up to maximum radius of  $r = 300$  au (Notsu *et al.* 2017).

Notsu *et al.* 2016). This is because the gas and dust temperatures, which are coupled in the midplane, are higher in the Herbig Ae disk than in T Tauri disk. We found that the abundance of H<sub>2</sub>O is high (up to  $10^{-4}$ ) in the inner region with higher temperature ( $\gtrsim 170\text{K}$ ) within  $\sim 7 - 8$  au, relatively high ( $\sim 10^{-8}$ ) between  $7 - 8$  au and  $14$  au (= the position of the H<sub>2</sub>O snowline,  $\sim 120\text{K}$ ) near the equatorial plane. In addition, it is relatively high ( $\sim 10^{-8} - 10^{-7}$ ) in the hot surface layer and the photodesorbed region of the outer disk, compared to its value ( $\sim 10^{-12}$ ) in the regions outside the H<sub>2</sub>O snowline near the equatorial plane (for more details, see Notsu *et al.* 2017).

There is the radial difference between the exact H<sub>2</sub>O snowline location ( $r \sim 14$  au) and the outer edge of the hot water vapor area ( $r \sim 8$  au) in a Herbig Ae disk, although there is no significant difference between them in a T Tauri disk with the radial steeper temperature profile in the disk midplane. It is because the water formation rate by gas-phase reactions strongly depends on the gas temperature. Such water vapor distribution in the Herbig Ae disk midplane was discussed in Woitke *et al.* (2009).

### 2.3. Calculations of H<sub>2</sub>O emission lines from protoplanetary disks

Using the H<sub>2</sub>O gas abundance distribution obtained from our chemical calculation described in the previous paragraph, we calculate the H<sub>2</sub>O emission line profiles ranging from near-infrared to sub-millimeter wavelengths from a T Tauri and a Herbig Ae disk assuming Keplerian rotation, and identify the lines which are the best candidates for probing emission from the inner thermally desorbed water reservoir, i.e., within the H<sub>2</sub>O snowline. In our work (e.g., Notsu *et al.* 2016, 2017), we adopted the same calculation method to determine the H<sub>2</sub>O emission line profiles from a T Tauri disk (based on Rybicki & Lightman 1986, Hogerheijde & van der Tak 2000, Nomura & Millar 2005, and Schöier *et al.* 2005), with the detailed model explained in Section 2.3 of Notsu *et al.* (2016). The code which we have built for calculating emission line profiles is a modification of

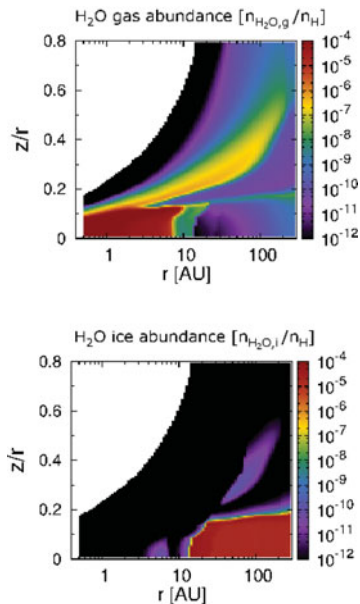


**Figure 2.** The fractional abundance (relative to total hydrogen nuclei density) distributions of  $\text{H}_2\text{O}$  gas (top) and  $\text{H}_2\text{O}$  ice (bottom) of a Herbig Ae disk as a function of disk radius and height (scaled by the radius,  $z/r$ ) up to maximum radius of  $r = 300\text{au}$  (Notsu *et al.* 2017).

the original 1D code called RATRAN<sup>‡</sup> (Hogerheijde & van der Tak 2000). We adopt the data of line parameters in the Leiden Atomic and Molecular Database LAMDA<sup>¶</sup> (Schöier *et al.* 2005). Here we note that in our method, we adopt the assumption of local thermal equilibrium (LTE) to obtain the level populations of the water molecule ( $n_u$  and  $n_l$ ). In addition, we set the ortho to para ratio (OPR) of water to its high-temperature value of 3 throughout the disk.

According to our calculations (e.g., Notsu *et al.* 2016, 2017), we showed that  $\text{H}_2\text{O}$  emission lines with small Einstein  $A$  coefficients ( $A_{ul} \sim 10^{-3} - 10^{-6} \text{ s}^{-1}$ ) and relatively high upper state energies ( $E_{\text{up}} \sim 1000\text{K}$ ) are dominated by emission from the region inside the  $\text{H}_2\text{O}$  snowline, and therefore their profiles potentially contain information which can be used to locate the position of the snowline. This is because the water gas column density of the region inside the  $\text{H}_2\text{O}$  snowline is high enough that all lines are optically thick as long as  $A_{ul} > 10^{-6} \text{ s}^{-1}$ . On the other hand, the region outside the  $\text{H}_2\text{O}$  snowline has lower water gas column densities and lines with larger Einstein  $A$  coefficients have a more significant contribution to their fluxes since the lines are optically thin. In addition, we calculated the profiles of lines which have been detected by previous spectroscopic observations using *Herschel* (e.g., the ortho- $\text{H}_2\text{O}$   $63.32\mu\text{m}$  and  $538.29\mu\text{m}$  lines). These lines are less suited to locate the position of the  $\text{H}_2\text{O}$  snowline, because they are not dominated in flux by the region inside the  $\text{H}_2\text{O}$  snowline.

Figure 3 shows the emission profiles of ortho- $\text{H}_2\text{O}$  lines at  $682.66\mu\text{m}$  ( $A_{ul} = 2.82 \times 10^{-5} \text{ s}^{-1}$ ,  $E_u = 1088.7\text{K}$ ),  $63.32\mu\text{m}$  ( $A_{ul} = 1.77 \text{ s}^{-1}$ ,  $E_u = 1070.6\text{K}$ ) and  $538.29\mu\text{m}$  ( $A_{ul} = 3.50 \times 10^{-3} \text{ s}^{-1}$ ,  $E_u = 61.0\text{K}$ ), for the Herbig Ae disk (Notsu *et al.* 2017). Figure 4 shows the line-of-sight emissivity (emissivity times extinction,  $\eta_{ul} e^{-\tau_{ul}}$ ; see Equation (14) of Notsu *et al.* 2016) along the line-of sight direction (from  $z = \infty$  to  $-\infty$ ) of the

<sup>‡</sup> <http://home.strw.leidenuniv.nl/michiel/ratran/>  
<sup>¶</sup> <http://home.strw.leidenuniv.nl/moldata/>

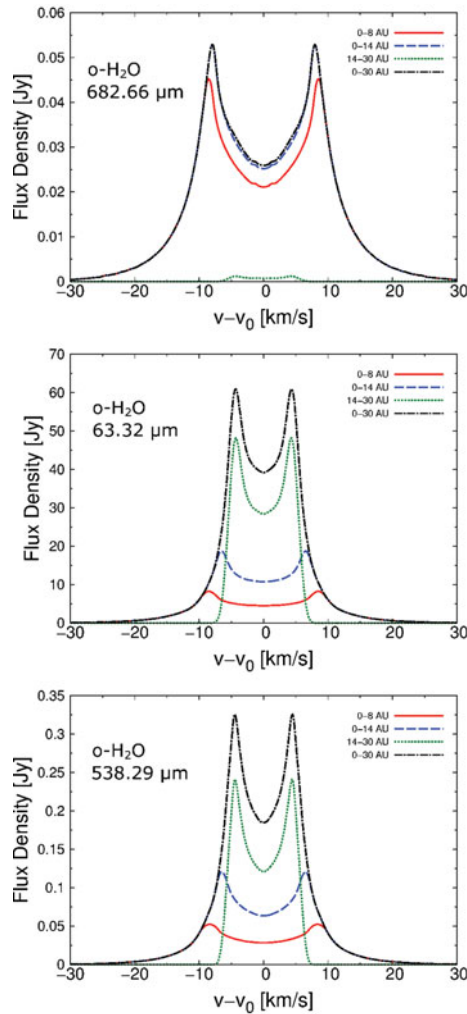


**Figure 3.** The emission profiles of ortho-H<sub>2</sub>O lines at 682.66 $\mu$ m (top), 63.32 $\mu$ m (middle) and 538.29 $\mu$ m (bottom), for the Herbig Ae disk. We assume that the distance to the object  $d$  is 140pc ( $\sim$  the distance of Taurus molecular cloud), and the inclination angle of the disk,  $i$ , is 30 degree (Notsu *et al.* 2017).

same three water lines for the Herbig Ae disk (Notsu *et al.* 2017). According to Figure 4, in the candidate 682.66 $\mu$ m line, the values of emissivity at  $r \lesssim 14$  au (= the position of the H<sub>2</sub>O snowline),  $T_g \gtrsim 120$ K, and  $z/r \sim 0.05 - 0.12$  are larger than those of the optically thin hot surface layer and the photodesorbed layer of the outer disk, and in particular those in the region with a higher H<sub>2</sub>O gas abundance ( $\sim 10^{-4}$ ,  $r < 7 - 8$  au, and  $T_g \gtrsim 170$ K) and  $z/r \sim 0.05 - 0.12$  are much larger.

Figure 5 shows the total fluxes of the various ortho-H<sub>2</sub>O lines which are the candidates for tracing emission from hot water vapor within the H<sub>2</sub>O snowline for a Herbig Ae disk (top panel) and a T Tauri disk (bottom panel) (Notsu *et al.* 2017). Since the fluxes of these lines from Herbig Ae disks are larger than those from T Tauri disks, the possibility of a successful detection is expected to increase for a Herbig Ae disk. The wavelengths of those lines which are the best candidates to locate the position of the H<sub>2</sub>O snowline range from mid-infrared to sub-millimeter. The values of total fluxes tend to be larger as

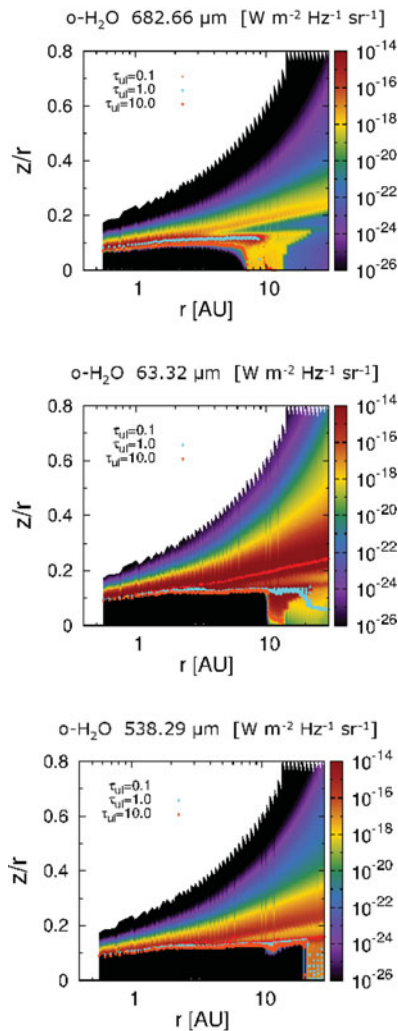


**Figure 4.** The line-of-sight emissivity of ortho-H<sub>2</sub>O lines at 682.66 $\mu$ m (top), 63.32 $\mu$ m (middle) and 538.29 $\mu$ m (bottom), for the Herbig Ae disk. In these panels, we overplot the total optical depth contours ( $\tau_{ul} = 0.1$  (red cross points), 1 (cyan circle points), and 10 (orange square points)) on top of these line emissivity panels (Notsu *et al.* 2017).

the wavelengths of the H<sub>2</sub>O lines become shorter. This is because the peak wavelength of the Planck function at the gas temperature around the H<sub>2</sub>O snowline ( $T_g \sim 100 - 200$  K) is in the mid-infrared region.

### 3. Discussion and Conclusion

In this work, we calculated the disk water vapor distribution and corresponding H<sub>2</sub>O line profiles for a T Tauri disk and a Herbig Ae disk, and identified candidate water lines which can locate the position of the H<sub>2</sub>O snowline across a wide wavelength range from mid-infrared to sub-millimeter.

The wavelengths of such candidate lines which trace emission from the hot water vapor within H<sub>2</sub>O snowline overlap with the capabilities of ALMA and future mid-infrared high-

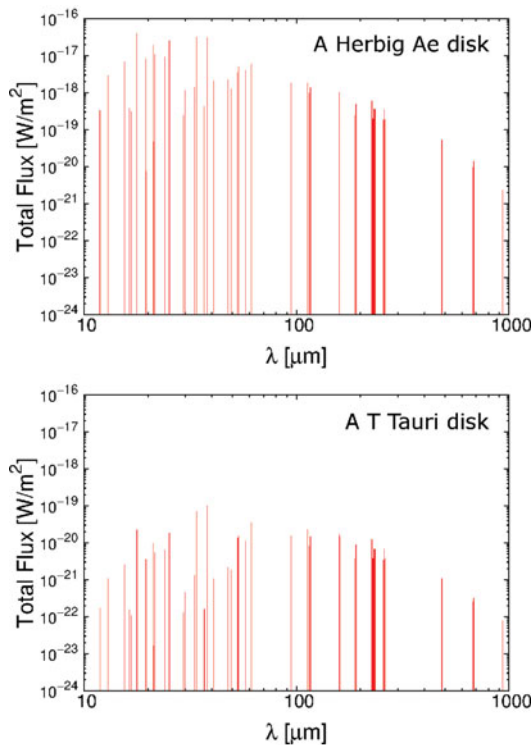


**Figure 5.** The total fluxes of the ortho-H<sub>2</sub>O lines which are best candidates to trace the emission from the water vapor within the H<sub>2</sub>O snowline, for a Herbig Ae disk (top panel) and a T Tauri disk (bottom panel) (Notsu *et al.* 2017).

dispersion spectrographs (e.g., SPICA/SMI-HRS). The successful detection in a Herbig Ae disk could be achieved with current ALMA capabilities using several lines. Mid-infrared instruments such as HRS on SPICA/SMI would have a high sensitivity in the Q band (e.g.,  $\sim 16\text{--}18\mu\text{m}$ ).

#### 4. Acknowledgements

The numerical calculations in this study were carried out on SR16000 at Yukawa Institute for Theoretical Physics (YITP) and computer systems at Kwasan and Hida Observatory (KIPS) in Kyoto University, and PC cluster at Center for Computational Astrophysics, National Astronomical Observatory of Japan. This work is supported by JSPS (Japan Society for the Promotion of Science) Grants-in-Aid for Scientific Research (Grant Number; 23103005, 25108004, 25108005, 25400229, 15H03646), by Grants-in-Aid for JSPS fellows (Grant Number; 16J06887), and by the Astrobiology Center Program of National Institutes of Natural Sciences (NINS) (Grant Number; AB281013). S. N. is grateful for the support from the educational program organized by Unit of Synergetic Studies for Space, Kyoto University. C. W. acknowledges support from the Netherlands Organization for Scientific Research (NWO, program number 639.041.335). Astrophysics at Queen's University Belfast is supported by a grant from the STFC (ST/P000312/1).

#### References

- Banzatti, A., Pontoppidan, K. M., Salyk, C., *et al.* 2017, *ApJ*, 834, 152
- Blevins, S. M., Pontoppidan, K. M., Banzatti, A., *et al.* 2016, *ApJ*, 818, 22
- Eistrup, C., Walsh, C., & van Dishoeck, E. F. 2016, *A&A*, 595, A83
- Furuya, K., Aikawa, Y., Nomura, H., Hersant, F., & Wakelam, V. 2013, *ApJ*, 779, 11
- Graedel, T. E., Langer, W. D., & Frerking, M. A. 1982, *ApJS*, 48, 321
- Hayashi, C. 1981, *Progress of Theoretical Physics Supplement*, 70, 35
- Hayashi, C., Nakazawa, K., & Nakagawa, Y. 1985, *Protostars and Planets II*, University of Arizona Press, 1100
- Heinzeller, D., Nomura, H., Walsh, C., & Millar, T. J. 2011, *ApJ*, 731, 115
- Hogerheijde, M. R., Bergin, E. A., Brinch, C., *et al.* 2011, *Science*, 334, 338
- Hogerheijde, M. R. & van der Tak, F. F. S. 2000, *A&A*, 362, 697
- Morbidelli, A., Bitsch, B., Crida, A., *et al.* 2016, *Icarus*, 267, 368
- Morbidelli, A., Chambers, J., Lunine, J. I., *et al.* 2000, *Meteoritics and Planetary Science*, 35, 1309
- Morbidelli, A., Lunine, J. I., O'Brien, D. P., Raymond, S. N., & Walsh, K. J. 2012, *Annual Review of Earth and Planetary Sciences*, 40, 251
- Nomura, H. & Millar, T. J. 2005, *A&A*, 438, 923
- Nomura, H., Aikawa, Y., Tsujimoto, M., Nakagawa, Y., & Millar, T. J. 2007, *ApJ*, 661, 334
- Notsu, S., Nomura, H., Ishimoto, D., Walsh, C., Honda, M., Hirota, T., & Millar, T. J. 2017a, *ApJ*, 836, 118
- Notsu, S., Nomura, H., Ishimoto, D., Walsh, C., Honda, M., Hirota, T., & Millar, T. J. 2016, *ApJ*, 827, 113
- Notsu, S., Nomura, H., Ishimoto, D., *et al.* 2015, *Revolution in Astronomy with ALMA: The Third Year*, ASP Conference Series, 499, 289
- Öberg, K. I., Murray-Clay, R., & Bergin, E. A. 2011, *ApJ*, 743, L16
- Oka, A., Nakamoto, T., & Ida, S. 2011, *ApJ*, 738, 141
- Okuzumi, S., Tanaka, H., Kobayashi, H., & Wada, K. 2012, *ApJ*, 752, 106
- Piso, A.-M. A., Öberg, K. I., Birnstiel, T., & Murray-Clay, R. A. 2015, *ApJ*, 815, 109
- Podio, L., Kamp, I., Codella, C., *et al.* 2013, *ApJ*, 766, L5
- Pontoppidan, K. M., Salyk, C., Blake, G. A., *et al.* 2010a, *ApJ*, 720, 887
- Pontoppidan, K. M., Salyk, C., Blake, G. A., & K&auml;luff, H. U. 2010b, *ApJ*, 722, L173
- Ros, K. & Johansen, A. 2013, *A&A*, 552, A137
- Rybicki, G. B. & Lightman, A. P. 1986, *Radiative Processes in Astrophysics*, by George B. Rybicki, Alan P. Lightman, pp. 400. ISBN 0-471-82759-2. Wiley-VCH, June 1986
- Sato, T., Okuzumi, S., & Ida, S. 2016, *A&A*, 589, A15
- Schöier, F. L., van der Tak, F. F. S., van Dishoeck, E. F., & Black, J. H. 2005, *A&A*, 432, 369
- van Dishoeck, E. F., Bergin, E. A., Lis, D. C., & Lunine, J. I. 2014, *Protostars and Planets VI*, University of Arizona Press, 835
- Walsh, C., Millar, T. J., & Nomura, H. 2010, *ApJ*, 722, 1607
- Walsh, C., Millar, T. J., Nomura, H., *et al.* 2014a, *A&A*, 563, AA33
- Walsh, C., Nomura, H., Millar, T. J., & Aikawa, Y. 2012, *ApJ*, 747, 114
- Walsh, C., Nomura, H., & van Dishoeck, E. 2015, *A&A*, 582, A88
- Woitke, P., Thi, W.-F., Kamp, I., & Hogerheijde, M. R. 2009b, *A&A*, 501, L5
- Woodall, J., Agúndez, M., Markwick-Kemper, A. J., & Millar, T. J. 2007, *A&A*, 466, 1197